

**Mo-99 2014 TOPICAL MEETING ON  
MOLYBDENUM-99 TECHNOLOGICAL DEVELOPMENT**

June 24-27, 2014  
Hamilton Crowne Plaza  
Washington D. C.

**Experimental Setup for Direct Electron Irradiation of the  
Uranyl Sulfate Solution: Bubble Formation and Thermal  
Hydraulics Studies**

Sergey Chemerisov, Roman Gromov, Vakho Makarashvili, Thad Heltemes, Zaijing Sun, Kent Wardle, James Bailey, Dominique Stepinski and George Vandegrift  
Argonne National Laboratory, 9700 South Cass Avenue, Argonne, IL 60439

**ABSTRACT**

Argonne is assisting SHINE Medical Technologies in developing SHINE, a system for producing fission-product  $^{99}\text{Mo}$  using a D/T-accelerator to produce fission in a non-critical target solution of aqueous uranyl sulfate. We have developed an experimental setup for studying thermal-hydraulics and bubble formation in the uranyl-sulfate solution to simulate conditions expected in the SHINE target solution during irradiation. A direct electron beam from the linac accelerator will be used to irradiate 20L solution volume (sector of the solution vessel). Because the solution will undergo radiolytic decomposition, we will be able to study bubble formation and dynamics and effects of convection and temperature on bubble behavior. These experiments will serve as a verification/validation tool for the thermal-hydraulic model. Utilization of the direct electron beam for irradiation allows homogenous heating of a large solution volume and simplifies observation of the bubble dynamics simultaneously with thermal-hydraulic data collection, which will complement data collected during operation of the mini-SHINE experiment. Irradiation will be conducted using a 30-40 MeV electron beam from the high-power linac accelerator. The total electron-beam power will be 20 kW, which will yield a power density on the order of 1 kW/L. The solution volume will be cooled by the front and back surfaces and by a central tube to mimic the geometry of the proposed SHINE solution vessel. Also, multiple thermocouples will be inserted into solution to map its thermal profiles.

**1. Introduction**

SHINE Medical Technologies is planning to use neutron-induced fission in a subcritical liquid target for production of Mo-99. During operation, the solution will undergo radiolytic decomposition. Formation of the bubbles, and their size and dynamics, will impact operational parameters of the liquid target, so an understanding of bubble behavior is critical for the ability to predict behavior of the salt solution during operation. In this experiment, we

are using the electron beam of the linear accelerator to irradiate a solution volume (sector of the solution vessel) to study the thermal hydraulics of the system. Experimental results obtained in this task will be compared with simulations to fine tune the computer model. Because the solution will undergo radiolytic decomposition from electrons slowing down in the liquid, we will be able to study bubble formation and dynamics and effects of convection and temperature on bubble behavior. These experiments will serve as a verification/validation tool for the thermal-hydraulic model. While data on radiolytic gas formation will be collected in mini-SHINE experiments, data for bubble-formation dynamics in mini-SHINE experiments will be limited due to the complexity of the optical setup for the extremely high radiation fields in the fissioning solution. Utilization of the direct electron beam irradiation allows homogenous heating of a large solution volume and simplifies simultaneous observation of the bubble dynamics with thermal-hydraulic data collection.

Irradiation will be conducted using a 30-40 MeV electron beam from the high-power linear accelerator. This range of electron-beam energy translates into 13-17 cm of an average range of electrons in water, so we can use a significantly large solution volume to see convective behavior resembling the bulk solution. The electron beam can be scanned and focused in such way that whole volume of the 15-cmx15-cmx80-cm solution is homogeneously heated. The total electron-beam power will be 20 kW, which will yield a power density on the order of 1 kW/L. This power can be uniformly distributed in the solution due to the low linear energy transfer (LET) of the high energy electrons. The beam-scan frequency will be high enough (up to 240Hz) to ensure uniform power distribution within the convection time constant of the solution.

The solution volume will be cooled by the front and back surfaces and by a central tube to mimic the geometry of the proposed SHINE solution vessel. Sides of the irradiation volume will be constructed out of quartz glass, so bubble formation and propagation can be observed using an ordinary camera. Also, multiple thermocouples will be inserted into the solution to map its thermal profiles.

According to literature data, gas generation due to electron radiolysis is expected to be four times less than that due to fission fragments, but we can vary the power density in the solution to make up for the difference in yield. We will combine bubble dynamic observation with gas generation measurements using a Residual Gas Analyzer (RGA), so we can establish a correlation between bubble dynamics and time required for establishing steady-state concentrations and onset of oxygen formation. We will irradiate water as well as an uranium salt solution to study thermal hydraulics of the system.

## **2. Design of the experimental apparatus**

The experimental setup for direct electron irradiation consists of the beam line and beam optics, the water-cooled solution chamber, a camera for bubble detection, and the cooling system. A schematic of the experimental setup is shown in Figure 1. Beam optics consist of a pair of quad magnets and pair of dipole magnets. This arrangement allows us to distribute the electron beam over the whole solution volume. The quad-magnet pair is used to control dimensions of the electron beam at the target, while the dipole pair is used to scan the beam in vertical and horizontal directions. A high-resolution camera is used to monitor formation

and movement of the bubbles in the solution. Because of the high radiation field near the solution volume, we have to use a mirror, so that the camera is not in the line of site of bremsstrahlung photons generated in target housing and solution. Our calculations showed that six inches of lead will be sufficient to shield the camera.

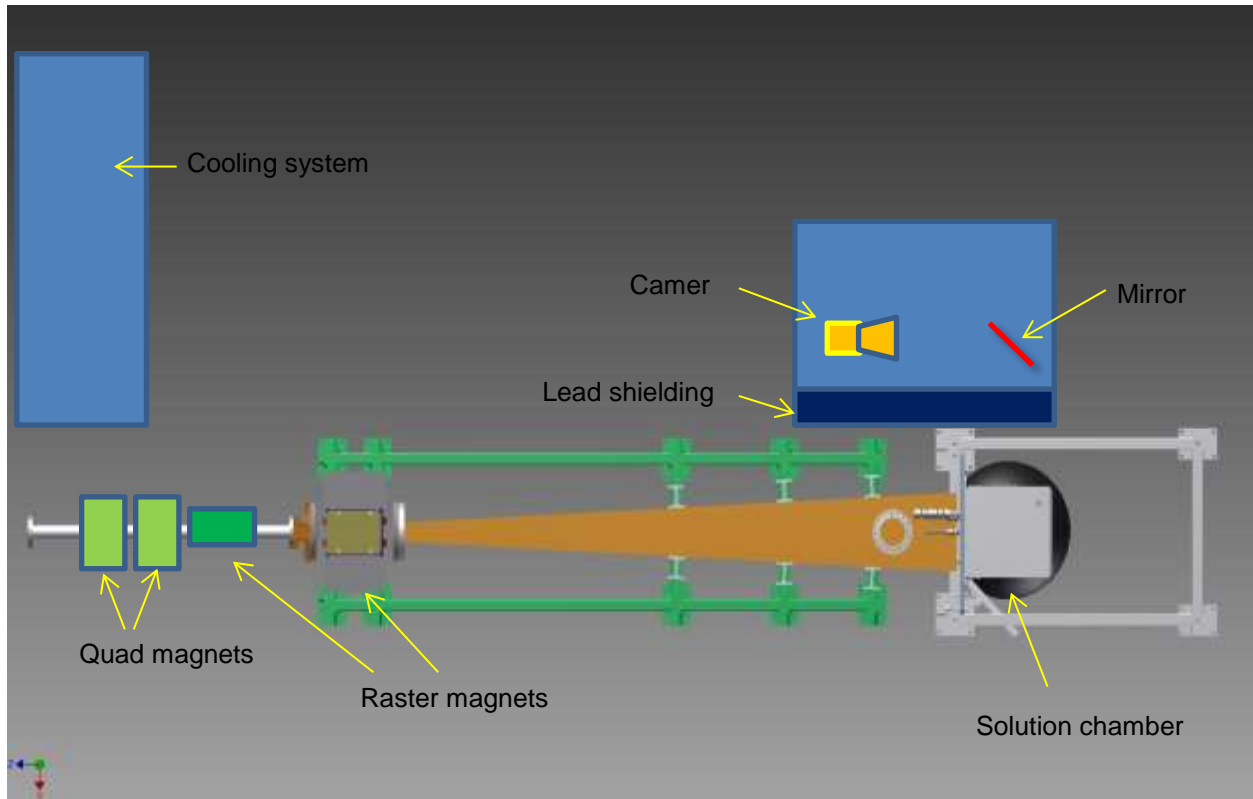


Figure 1. Layout of the experimental setup.

Details of the chamber assembly are shown in the Figure 2. The assembly contains a rectangular sealed vessel that contains the uranyl-sulfate solution. The electron beam enters the vessel through a beam window located at the left-side wall. The outer surface of this wall interfaces with the raster vacuum chamber in the beam line. There is an o-ring seal at this interface. The beam window is double walled to allow for coolant flow between the walls. Also, the thickness of these walls has been minimized to reduce the loss of the beam in the wall material. The two side walls have quartz windows for visual inspection of the solution during irradiation. The right side wall as well as the bottom wall is doubled-walled to also provide for coolant flow. In addition, there is a drain and fill tube connection in the bottom wall of the vessel. The vessel's top plate contains penetrations for thermocouple assemblies, a coolant center tube, and additional penetrations for venting and purging. The chamber is a welded all stainless steel construction. The pressure in the vessel will be kept sub-atmospheric. Sweep gas (helium) will be introduced into the head space of the chamber. The flow rate of the cover gas will be adjustable so the concentration of the radiolytically produced hydrogen will be maintained below one percent. The sweep gas will be collected in gas collection system of the mini-SHINE experiment. The composition of the gas will be

continually monitored by a gas monitoring system. This will allow us to measure radiolytic gas generation rates. The solution chamber is equipped with seven thermocouple assemblies, each having six measuring points, so we will be able to measure temperature of the solution in 42 points simultaneously.

A secondary chamber (Figure 2b) is installed around the solution chamber in order to mitigate a containment failure of the primary vessel. The left side-wall of the secondary chamber interfaces with the inside surface of the primary left side (beam side) plate and is sealed using an o-ring. The side walls have quartz windows to allow observation of the bubbles in the solution. These windows are aligned with the primary windows. A two inch drain is located in the bottom of the chamber and is connected to an external holding tank. The secondary containment is not intended to hold the entire inventory of the process fluid. Therefore, any leakage into the secondary must be free to drain to the holding tank. Also, there is a vent in the top plate of the secondary chamber that is connected to the process exhaust system, causing the secondary to have a slightly negative pressure relative to the room pressure. The secondary containment is welded aluminum construction.

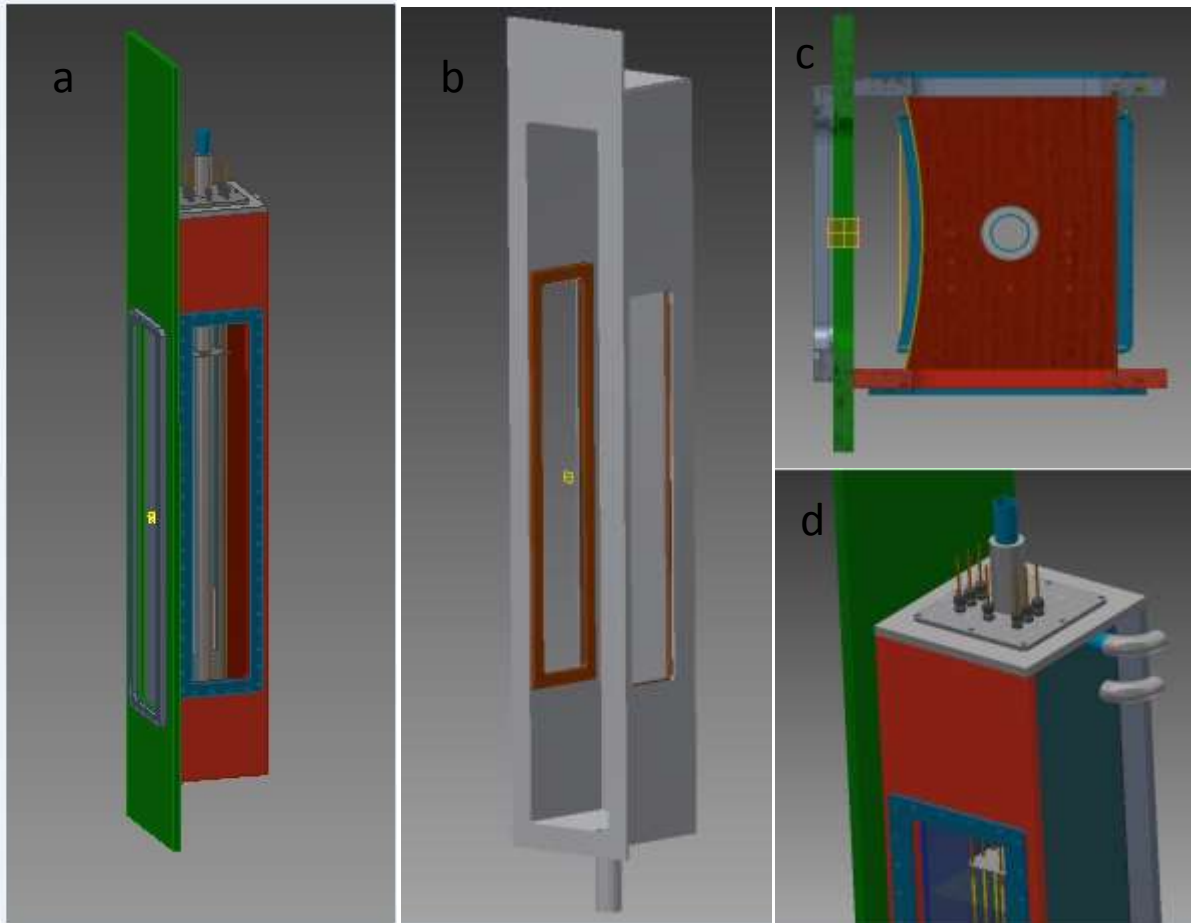


Figure 2. A detailed view of the solution chamber; **a.** Main solution chamber. **b.** Secondary aluminum enclosure. **c.** Top view of the main solution chamber. **d.** Close-up view of the top portion of the main solution chamber showing position of the central cooling tube and penetrations for thermocouple assemblies

The cooling system for the experiment is designed to have sufficient capacity to remove 20 kW of heat. A cooling-water pump is sized to provide 50 gpm of water flow at up to 50 psig pressure. The cooling system has an all welded design. All components are stainless steel and equipped with mixed-bed deionizer to remove possible contaminants from the cooling water. The head space of the make-up tank is purged by air and is vented through the HEPA equipped exhaust system to prevent hydrogen buildup. All elements of cooling system that are not welded are located inside an enclosure to prevent spread of suspect coolant water to the environment. This enclosure is also connected to the HEPA equipped exhaust system.

### 3. Computational fluid dynamics simulations

We have used two different Computational Fluid Dynamics (CFD) simulation packages to calculate temperature in the irradiated solution, and preliminary multiphase CFD simulations were conducted using a custom solver built in the OpenFOAM CFD toolkit (version 2.1.x) based on the Eulerian-Eulerian multi-fluid methodology [1] with additional capability for sharp interface capturing (*multiphaseEulerFoam* solver). Solution of the energy transport equation along with density variations using the Boussinesq approximation were also incorporated into the solver. 2D and 3D simulations for a box 15cm x 15cm x 1m (with 80cm of liquid and a 20cm headspace) were performed. Simulations were done using a uniform volumetric heat generation rate of 20kW as well as using a block averaged profile (in the beam penetration direction) taken from Monte Carlo particle transport code calculations (MCNPX) with a total generation rate of 15kW. Wall temperature was held at 20C. For this first set of simulations, rather than as a volumetric source proportional to the volumetric heat generation, the introduction of the radiolytically produced gas was from the inner wall with a flow rate equivalent to a volume fraction of 1% (1.5 ml/s); a bubble size of 1mm was assumed and a virtual mass coefficient of 0.5 was used. The properties of the gas phase were taken as the stoichiometric average of hydrogen and oxygen. The influence of the introduction surface for gas bubbles (bottom versus side) was explored and found to have minimal influence. As the flow in these conditions is expected to be in the turbulence transition regime, the role of turbulence modeling was also expected to be important and was explored with the use laminar flow assumption and fully-transient large eddy simulation (LES) (using the Smagorinsky sub-grid model [2]).

It was found that the negative impact of the thermal conductivity of the gas phase had a significant influence on the overall temperature profiles much more than the convective flow magnitudes (and correspondingly the assumed droplet size). While the upper free surface of the liquid was included in the model, it was found that motion of the liquid surface was not substantial; however, it was noticed that currents in the gas headspace, which develop quickly, did have an important influence on the initial development of natural convection loop in the upper section of the liquid volume. Additionally, the role of turbulence was found to be critically important to the overall heating; the maximum temperature of the fluid volume was found to increase much more significantly when laminar flow is assumed as compared to turbulent flow using LES. Moreover, the details of the treatment of wall boundaries in regards to heat transfer in the boundary layer were also found to be of importance.

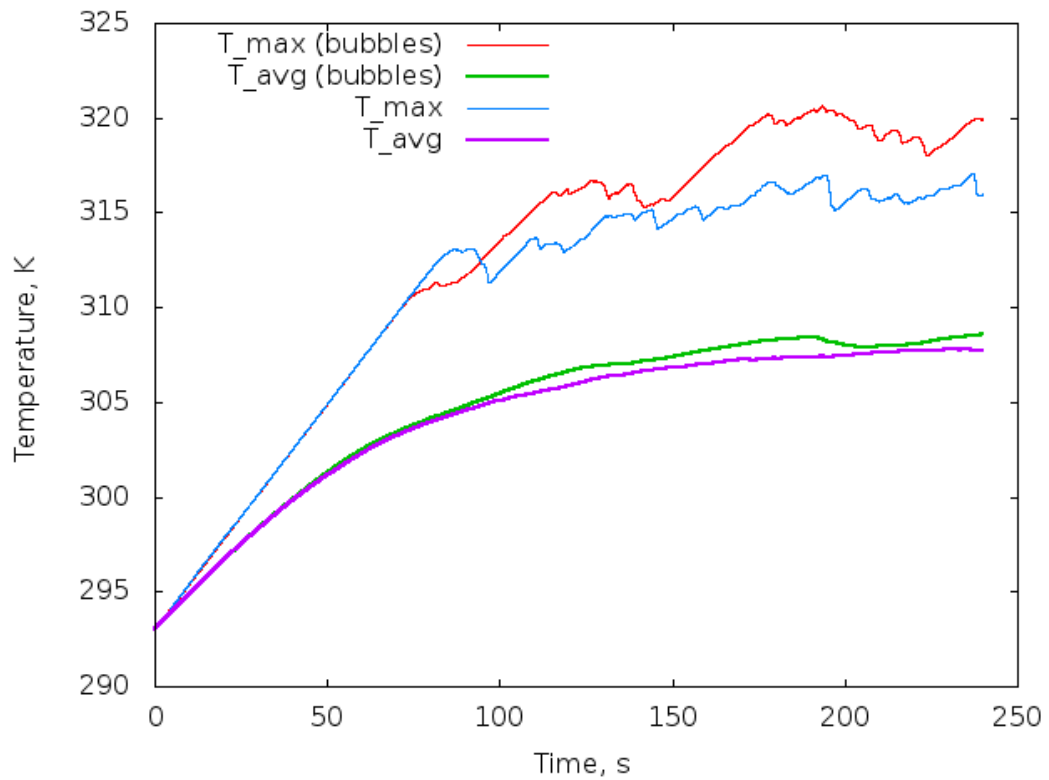


Figure 3. Maximum and average temperature of the solution with and without bubbles present.

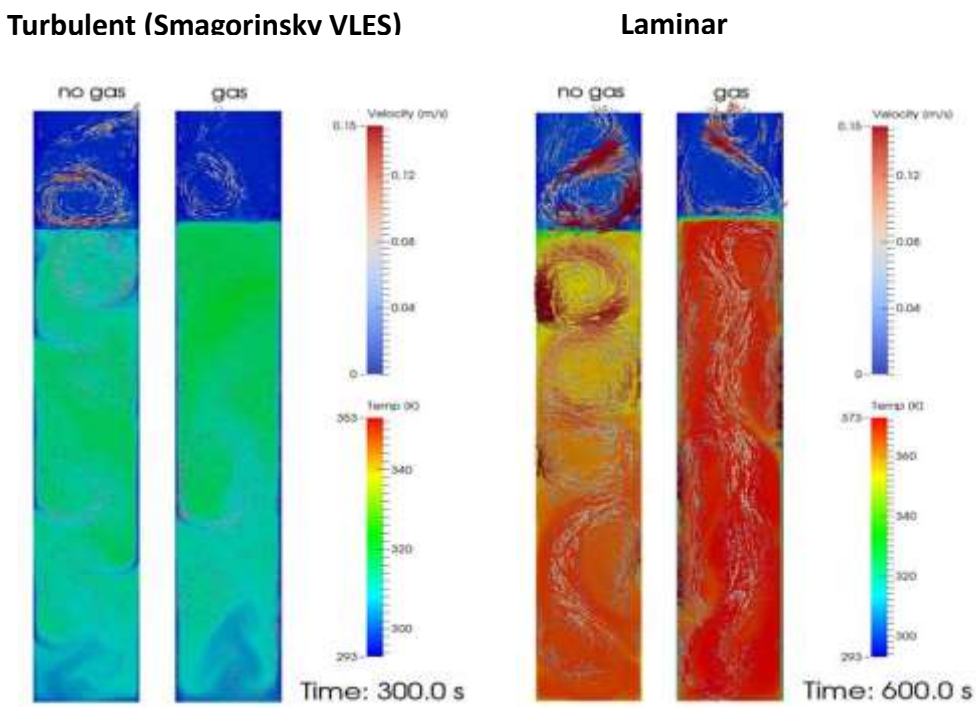


Figure 4. Flow velocity and temperature distribution for solution chamber under irradiation.

We have also performed hydraulic analysis of the process fluid under irradiation using an ANSYS CFX computer code. For these simulations we assumed a rectangular fluid volume with a 10kW uniform heat generation due to beam heating. The boundary at the left, right and bottom walls (walls that are force convected cooled) were assumed to be at a constant near ambient temperature (I.e. coolant temperature). The two side walls (walls with no cooling and with viewing windows) were assumed insulated. Also, the free surface at the top of the process fluid was assumed insulated. The process fluid properties were assumed to be that of water.

The temperature and velocity profiles through the center of the chamber are shown on Figure 5. The maximum temperature in the fluid is 81°C at the 10kW heat generation rate. Essentially, the analysis indicates that a heat generation significantly above the 10kW would result in boiling in the fluid. The velocity profile shows the weak natural convection flow within the fluid. The resulting high thermal convective resistance inherently limits the maximum beam power for irradiation of the fluid. Two computer models yield quite different results; ultimately experimental measurements will provide information to verify computer model.

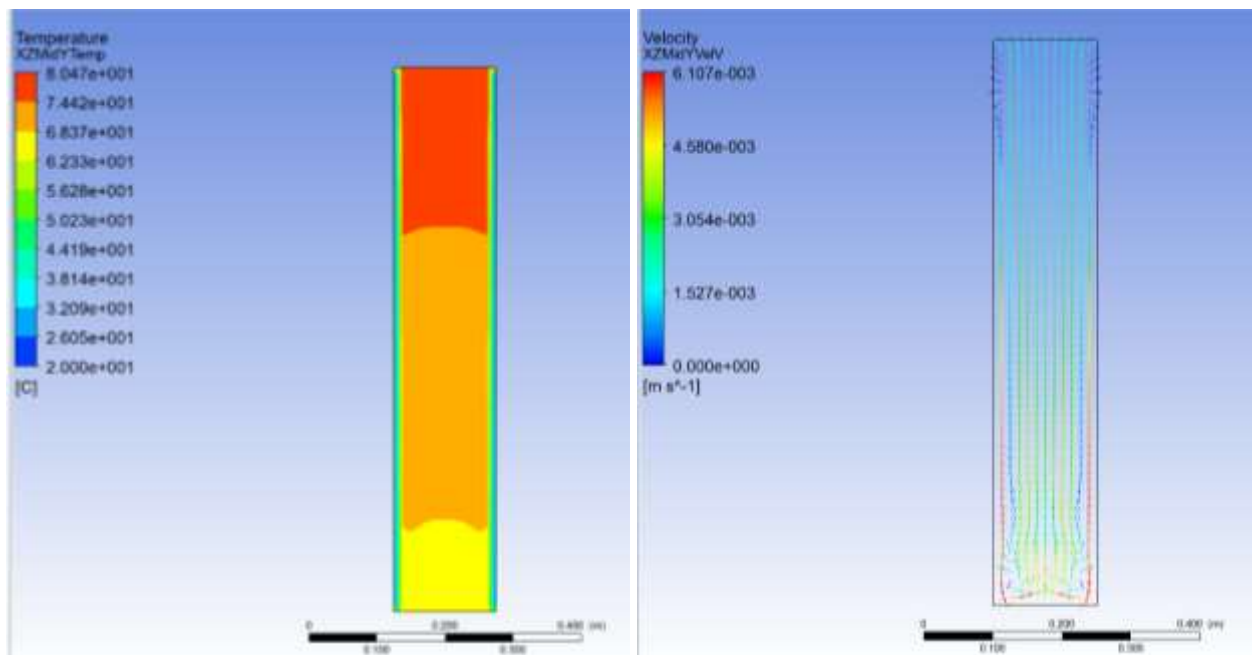


Figure 5. Temperature and velocity profiles for 20 L solution volume. Power deposition in solution is 10kW.

#### 4. Engineering Design Analyses

A structural analysis of the electron beam raster vacuum chamber was performed using ANSYS Mechanical15.0 software. The model utilized quarter symmetry and assumed 1 atm

of external pressure. The initial design of the chamber incorporated 3/8" thick 6061 aluminum walls. Initial analysis of the vacuum chamber indicated that additional structural elements were necessary to reduce both mechanical stress and distortion from external pressure. The first iteration of adding structural elements is shown below (Figure 6) on the left with 4 structural tees, and on the right is the quarter symmetric model with external pressure applied.

The stress and deflection plots for the chamber are shown on the Figure 6 (bottom two depictions). The maximum stress in the chamber is 17.3 kpsi at the end of a tee where the top wall meets the side wall. The maximum deflection occurs in the side wall with a value of 2.4 mm. The final results led to a design with 3/8" thick plates plus 6 additional I-beam elements to reduce stress and deflection to 10,000 psi and 1.4 mm respectively.

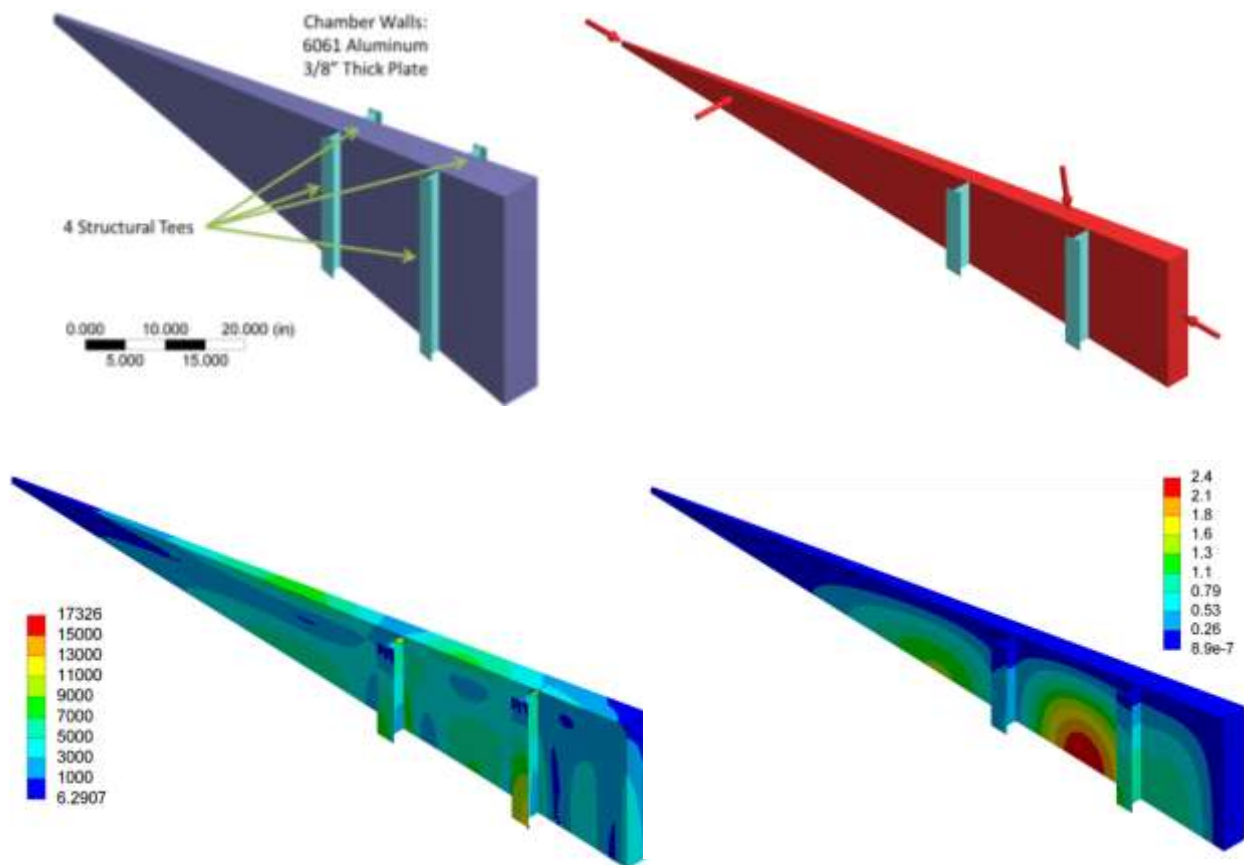


Figure 6. Design and results of the stress analysis vacuum raster chamber.

The large size of the water-cooled beam window and our desire to minimize material thicknesses, which cause beam losses, represented a significant engineering challenge. The solution we found included a curved window to resist the buckling. Static structural analysis of the beam window separating the electron beam and the process fluid was performed using

an ANSYS computer model. The window uses a double-wall design to allow coolant flow, as well. The window design employs a 15 inch cylindrical radius to maintain the necessary rigidity while minimizing material thickness. The side towards the vacuum chamber must resist a pressure differential of 24.7 psi.

Initial results from the analysis showed that the main concern in the window design would be the ability to provide sufficient rigidity to resist buckling. A linear buckling analysis was performed based on the static structural analysis, and the design was adjusted to withstand buckling from a differential pressure of 50 psi. However, during leak testing of the window assembly tendency to buckle was observed probably due to deformation of the windows during fabrication, which necessitated supplemental stiffening with 6 ribs. The real curvature of the window was measured and each rib was cut to precisely reflect this curvature. Those ribs were welded to the vacuum side of the window assembly. Consecutive testing of the window assembly showed not buckling.

### 5. Monte Carlo simulations

Monte Carlo simulations were conducted using the MCNPX computer code[3]. The geometry used in calculations is shown on Figure 7. The main contributor to the dose around the setup is activation of the uranium solution. The exposure rates at different distances and different cool-down times are summarized in Table 1.

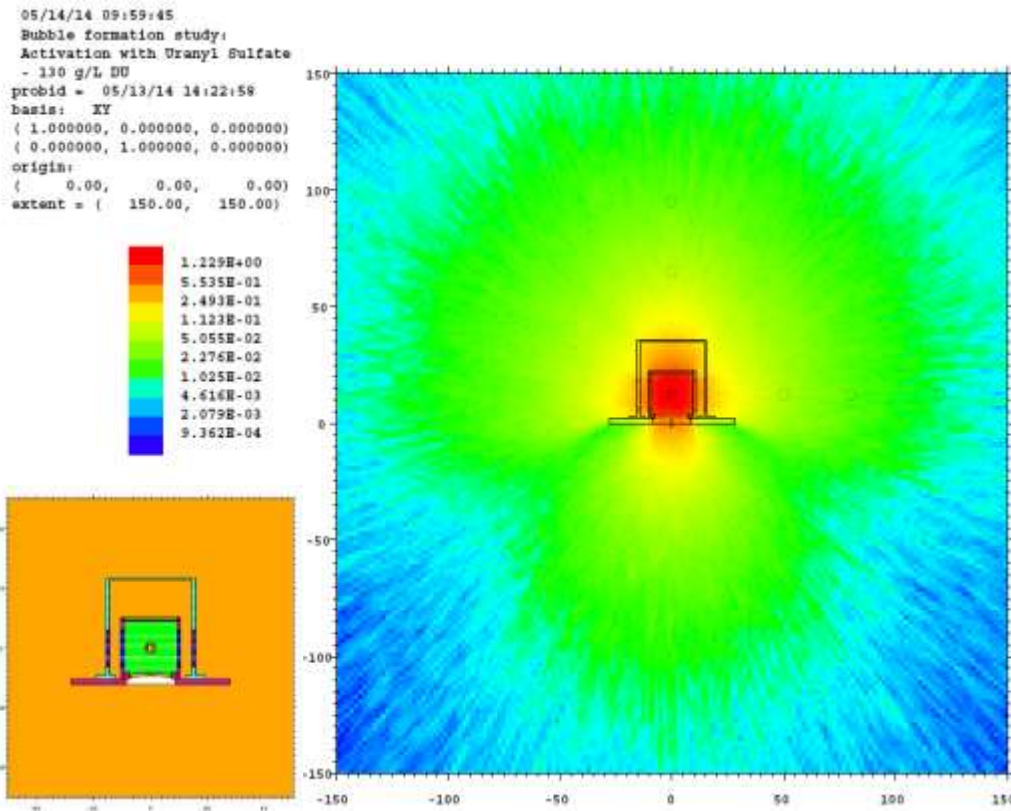


Figure 7. Geometry of the solution chamber used in MNCPIX calculations and dose distribution around the setup after irradiation for 1 hour at 10kW beam power and twelve hours cool down time.

Table 1. Exposure rates for the irradiated DU solution in the process vessel after 1 hour irradiation at 10 kW beam power.

	<b>Beam axis - Y</b>		
	<u>12 hours post EOB</u>	<u>1 day post EOB</u>	<u>1 week post EOB</u>
<u>Distance[cm]</u>	<u>Exposure Rate[R/hr]</u>		
30	5.83E-02	3.16E-02	3.76E-03
60	2.57E-02	1.32E-02	1.52E-03
100	1.14E-02	6.69E-03	9.06E-04
	<b>Perpendicular to beam axis - X</b>		
	<u>12 hours post EOB</u>	<u>1 day post EOB</u>	<u>1 week post EOB</u>
<u>Distance[cm]</u>	<u>Exposure Rate[R/hr]</u>		
30	4.88E-02	2.34E-02	3.08E-03
60	2.17E-02	1.05E-02	1.54E-03
100	9.49E-03	4.51E-03	6.01E-04

## 6. Summary

We have designed and are fabricating an experimental apparatus for direct electron beam irradiation of uranyl sulfate solution. This experimental setup will allow observation of radiation-induced bubble formation in the solution as well as measurements of the gas evolution. Installation of the experimental setup is already started and experiments will start in July 2014.

## 7. References

- [1] K. E. Wardle and H. Weller, "Hybrid Multiphase CFD Solver for Coupled Dispersed/Segregated Flows in Liquid-Liquid Extraction," *Int. J. of Chem. Eng.* 2013, 128936 (2013).
- [2] Pope, Stephen (2000). Turbulent Flows. Cambridge University Press.
- [3] D. Pelowitz, ed., "MCNPX User's Manual, Version 2.7.0", LA-CP-11-00438, Los Alamos National Laboratory (April 2011).

## Acknowledgement

Work supported by the U.S. Department of Energy, National Nuclear Security Administration's (NNSA's) Office of Defense Nuclear Nonproliferation, under Contract DE-AC02-06CH11357. Argonne National Laboratory is operated for the U.S. Department of Energy by UChicago Argonne, LLC.